



Fully-developed compartment fire dynamics in large-scale mass timber compartments

Ian Pope^{a,b,*}, Vinny Gupta^{a,c}, Hangyu Xu^a, Felix Wiesner^d, David Lange^a, José L. Torero^e, Juan P. Hidalgo^a

^a The University of Queensland, School of Civil Engineering, Brisbane, Australia

^b DBI – The Danish Institute of Fire and Security Technology, Denmark

^c The University of Sydney, School of Aerospace, Mechanical and Mechatronic Engineering, Sydney, Australia

^d The University of British Columbia, Department of Wood Science, Vancouver, Canada

^e University College London, Department of Civil, Environmental and Geomatic Engineering, London, UK

ARTICLE INFO

Keywords:

Compartment fires
Fire dynamics
Heat transfer
Large-scale
Mass timber
Cross-laminated timber

ABSTRACT

A series of large-scale experiments has been conducted on under-ventilated mass timber room compartments with kerosene pool fires. To characterise the role of exposed timber walls on the fully-developed phase of the fire, the exposed surface area of mass timber was varied between experiments. Experiments with all timber surfaces protected were compared against compartments with the ceiling and one or two walls exposed. The results show that increasing the surface area of exposed timber alters the flow fields both inside the compartment and at the doorway. The momentum-driven flow fields control the spatial distribution of temperatures, surface heat fluxes, and the neutral plane. Temperatures, heat fluxes and velocities within the compartment are shown to be spatially heterogeneous in both horizontal and vertical planes, highlighting the complexity of the flow fields. This represents a significant divergence from the conventional assumptions for under-ventilated compartments of minimal velocities and homogeneous thermal conditions governed by the opening factor. The results demonstrate that the momentum-driven flow fields created by the burning walls control the compartment fire dynamics. Therefore, typical simplifications of the momentum equation in zone models are not valid for mass timber compartments, and these solutions should only be used in a conservative manner.

1. Introduction

As enthusiasm for tall timber buildings has grown, there has been a significant increase in fire experimentation involving large-scale timber compartments [1–8]. Many of these experiments have involved compartment geometries that are representative of under-ventilated, or ‘Regime I’, fire conditions [9] – typical of residential buildings. Within this regime, the internal fire dynamics for the fully-developed compartment fire are independent of the fuel load nature and the compartment linings (combustible vs non-combustible). Instead, the fire dynamics are controlled by the compartment geometry and openings, which govern the rate of oxygen transport to the fire [10]. These factors are especially important for timber structures, since the fire dynamics govern heat exposure and the potential for self-extinction of the exposed timber surfaces after burnout of the moveable fuel load [2–5,11], as well as the performance of encapsulation systems [12] and other

non-combustible elements. Appropriate design methodologies and failure criteria associated with these variables are being developed through an ongoing study involving a series of large-scale experiments [13,14] on under-ventilated room compartments with different moveable fuel loads and numbers of exposed surfaces. As part of this study, the aim of this paper is to analyse the internal fire dynamics during the fully-developed phase of these experiments, and to characterise the influence of the configuration and extent of exposed combustible timber surfaces. The external fire dynamics are of equal importance but are beyond the scope of this study.

Despite the number of experiments that have been carried out and reviewed [15], there remains a lack of the data required to characterise the internal fire dynamics in timber compartments, such as incident heat fluxes, velocities, and gas species concentrations. Large-scale experiments in under-ventilated compartments with non-combustible linings have exhibited wide ranges of spatial distribution in temperature and

* Corresponding author. The University of Queensland, School of Civil Engineering, Brisbane, Australia.

E-mail addresses: ian.pope@uqconnect.edu.au, ipo@dbigroup.dk (I. Pope), vinny.gupta@sydney.edu.au (V. Gupta), felix.wiesner@ubc.ca (F. Wiesner).

<https://doi.org/10.1016/j.firesaf.2023.104022>

Received 13 June 2023; Received in revised form 30 September 2023; Accepted 5 October 2023

Available online 6 October 2023

0379-7112/© 2023 The Authors. Published by Elsevier Ltd. This is an open access article under the CC BY license (<http://creativecommons.org/licenses/by/4.0/>).

heat flux, which are due to complex interactions between compartment geometry, opening size, boundary linings and fuel characteristics [10, 16]. This highlights the importance of achieving a sufficient resolution of instrumentation within the compartment to characterise the relevant phenomena and representative thermal boundary conditions [10].

Key assumptions of *Regime I* compartment fires are that momentum within the enclosure is negligible, and that the thermal environment within is approximately homogeneous [9]. These characteristics are also fundamental to the validity of zone models [17,18] that calculate average gas temperatures within a hot smoke layer or zone that is assumed to be well-mixed. However, it has been shown for compartments at the medium-scale that introducing burning walls promotes momentum-driven flow fields [11], which control the fuel burning rate and spatial distribution of energy release, and are highly sensitive to the coupling of the fuel and compartment geometry [19]. This interaction is expected to be considerably more complex at larger scales, but the influence of scale and exposed timber area has not been studied systematically. This paper addresses this by characterising the fully-developed fire dynamics and surface thermal exposures of multiple large-scale timber compartment fire experiments with varying configurations of exposed timber surfaces. Section 3 describes the fire regime within each compartment, through analysis of the internal temperature and velocity fields, while Section 4 relates this to the measured heat fluxes to the boundaries. Finally, Section 5 explains the significance of these results for the design and analysis of mass timber buildings.

2. Experimental set-up

A series of large-scale fire experiments in cross-laminated timber (CLT) compartments have been conducted by the authors in the development of a self-extinction design framework for mass timber [13]. These compartments were of $3.15 \text{ m} \times 3.15 \text{ m} \times 2.70 \text{ m}$ internal dimensions, with a single opening 0.85 m wide and 2.10 m high. The CLT panels were 125 mm thick, comprising three layers of $45\text{--}35\text{--}45 \text{ mm}$ thick radiata pine, glued with Purbond HBS polyurethane adhesive. The internal height of the compartment was reduced from 3.0 m to 2.7 m by the inclusion of a non-combustible false floor to protect the instrumentation below from the heat of the fire. After accounting for the additional thickness of encapsulation boards, the inverse opening factors of the compartments ranged between 17.2 and $17.6 \text{ m}^{-1/2}$, corresponding to *Regime I*. This geometry is representative of residential-style building occupancies, which are typically associated with ventilation-controlled fires. The CLT walls and ceiling were either fully encapsulated (Test 1.1 and Test 1.2), or partially encapsulated with one wall and the ceiling exposed (Test 2.1 and Test 2.2), or partially encapsulated with two walls and the ceiling exposed (Test 3.1). The specific characteristics of each experiment are summarised in Table 1, including the ratio of exposed timber surface area, A_e , to the total compartment surface area (not including the opening), A_T . The encapsulation consisted of two layers of 13 mm thick fire-rated plasterboard attached to the CLT with screws.

The fuel load in the experiments was provided by a continuously fed kerosene pool located in the centre of the room. The kerosene pool of $1000 \text{ mm} \times 1000 \text{ mm} \times 100 \text{ mm}$ was used to control the fuel load in the compartment through a re-filling tray system similar to those described by Gorska et al. [11] and Tondini and Franssen [20]. This allowed the

duration of burning of the 'moveable' fuel load to be controlled to either induce or prevent char fall-off and encapsulation failure. For two of the experiments (Test 1.1 and Test 2.1), the fuel supply to the pool was sustained until these critical events occurred and beyond, for a duration of more than 30 min , after which the fuel supply was cut. Based on the outcomes of these 'long' duration fires, Test 1.2 was designed with a shorter pool fire duration of approximately 10 min (post-flashover) to prevent any encapsulation failure. Similarly, Test 2.2, with two exposed surfaces, was designed with a pool fire duration of approximately 15 min (post-flashover) to narrowly avoid char fall-off and demonstrate or investigate self-extinction occurrence upon burnout of the pool after the supply was shut-off. This pool fire duration was subsequently repeated for Test 3.1 with three exposed surfaces, which did not self-extinguish. The kerosene pool and inside of the compartment are shown in Fig. 1, while further details of the compartment and instrumentation are given in Ref. [13].

As shown in Fig. 1, the compartment walls and ceiling were labelled from A to E, where A was the front wall (featuring the opening and not visible in the figure) with B and D on either side and C at the back. In Test 2.1 and Test 2.2, wall D and the ceiling E were exposed with all other surfaces encapsulated, while in Test 3.1 wall B was also exposed. Measurements of gas-phase temperatures and incident heat fluxes to the boundaries were taken using a high density of instrumentation – including up to 43 thermocouples, and 61 thin-skin calorimeters (TSCs) [21].

At a minimum, all of the experiments included five thermocouple (TC) trees distributed around the compartment as shown in Fig. 2 (a), each with seven thermocouples spaced at 338 mm height intervals between the false floor and the ceiling. An additional eight TCs were distributed along the height of the opening, corresponding to the locations of eight bi-directional velocity probes (BDPs), as shown in Fig. 3 (a). A further three internal BDPs were fixed at different heights on the back wall of the compartment, shown in Fig. 3 (b), to measure the vertical velocities near the back wall. The thermocouples used were 1.5 mm diameter type K Inconel-sheathed thermocouples with insulated junctions, except in Test 3.1, where 3.0 mm thermocouples were used. Thicker thermocouples were used in this test for greater robustness, as many of the thermocouples in previous tests were eventually destroyed by the extended periods of heating above 1100°C . The increased diameter may result in a slightly longer response time (less than 1 s), but this delay is of no significance for these particular experiments. In contrast, the diameter could have an effect on the temperatures recorded. In areas where the soot volume fraction is high, the thermal equilibrium temperature will not be a function of the diameter. Nevertheless, in areas of low soot concentration the increased diameter will result in higher radiative influence on the measurements. Thus, temperatures recorded will be higher. The value of temperature measurements in cold areas is mostly qualitative (to establish the smoke/air interface) so this difference will not be significant. As a result, no radiation correction was applied to the temperature results due to the significant assumptions required of the optical environment in the compartment [22].

The TSCs were installed on the walls and ceiling to measure the incident heat fluxes on the internal compartment boundaries. Fig. 2 (b) shows the placement of TSCs on each surface. The TSCs, which were embedded flush with the compartment surfaces, were constructed from

Table 1
Characteristics of each experiment.

Name	Duration	Exposed CLT surfaces	Exposure ratio (A_e/A_T)
Test 1.1	Long	None (all encapsulated)	0
Test 1.2	Short	None (all encapsulated)	0
Test 2.1	Long	Two – ceiling (E) and one side wall (D)	0.35
Test 2.2	Short	Two – ceiling (E) and one side wall (D)	0.35
Test 3.1	Short	Three – ceiling (E) and two side walls (B & D)	0.52

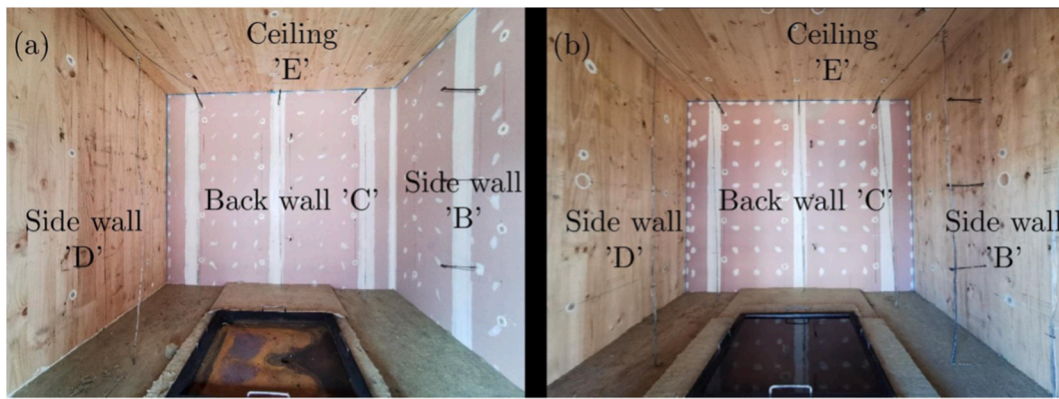
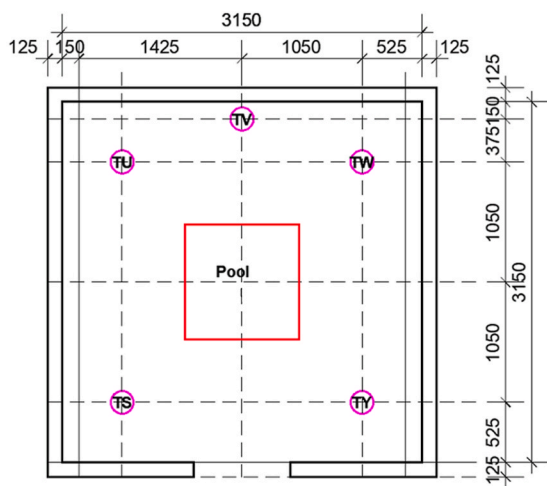
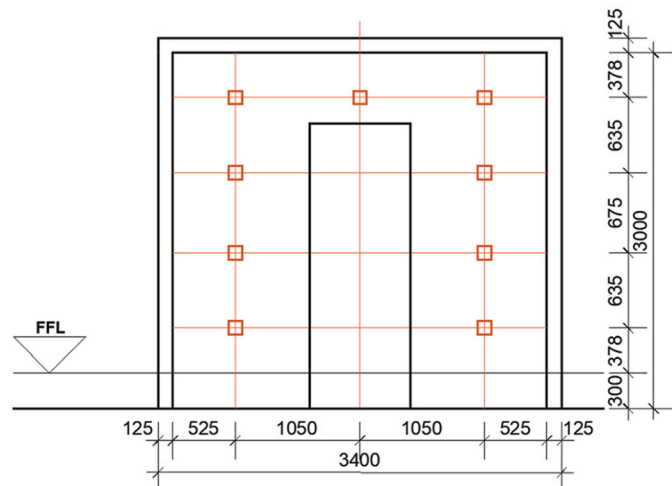


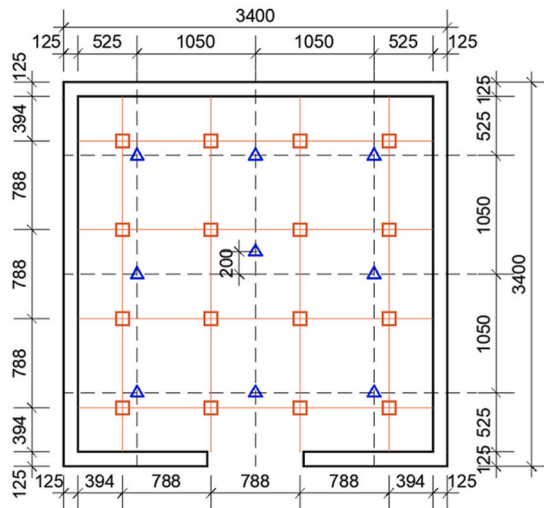
Fig. 1. Compartment with (a) two exposed surfaces in Test 2.1 and Test 2.2, and (b) with three exposed surfaces in Test 3.1 [13].



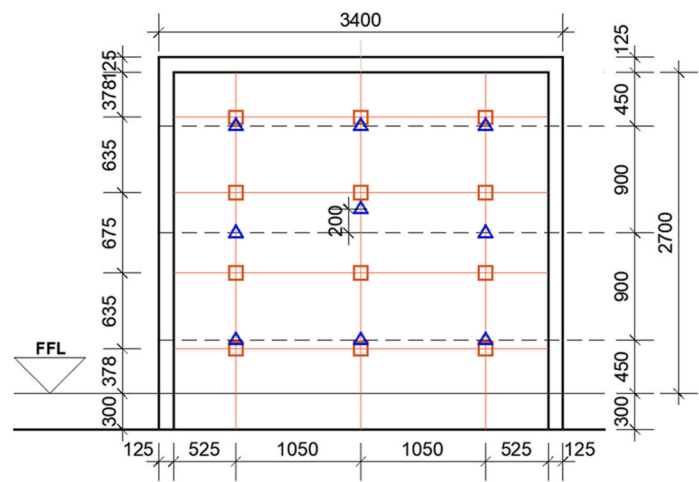
(a) Plan View and TC Trees



(b.1) Front Wall TSCs



(b.2) Ceiling TSCs



(b.3) Side and Back Wall TSCs

Fig. 2. Locations of (a) gas-phase thermocouple trees (seven TCs per tree), and (b) thin-skin calorimeters on encapsulated surfaces (brown squares) and exposed surfaces (blue triangles). (For interpretation of the references to colour in this figure caption, the reader is referred to the Web version of this article.)

50 mm diameter and 40 mm thick vermiculite cylinders, with a 10 mm diameter and 1 mm thick Inconel disc in the centre. Further detail on the design and calibration of the TSCs used in these experiments can be found in Ref. [13].

The use of instrumentation in these experiments followed the approach of several other studies [13,21–26], which further discuss the validity and uncertainty of the different measurement techniques. The TSCs used have been calibrated for radiant heating exposures [21], so

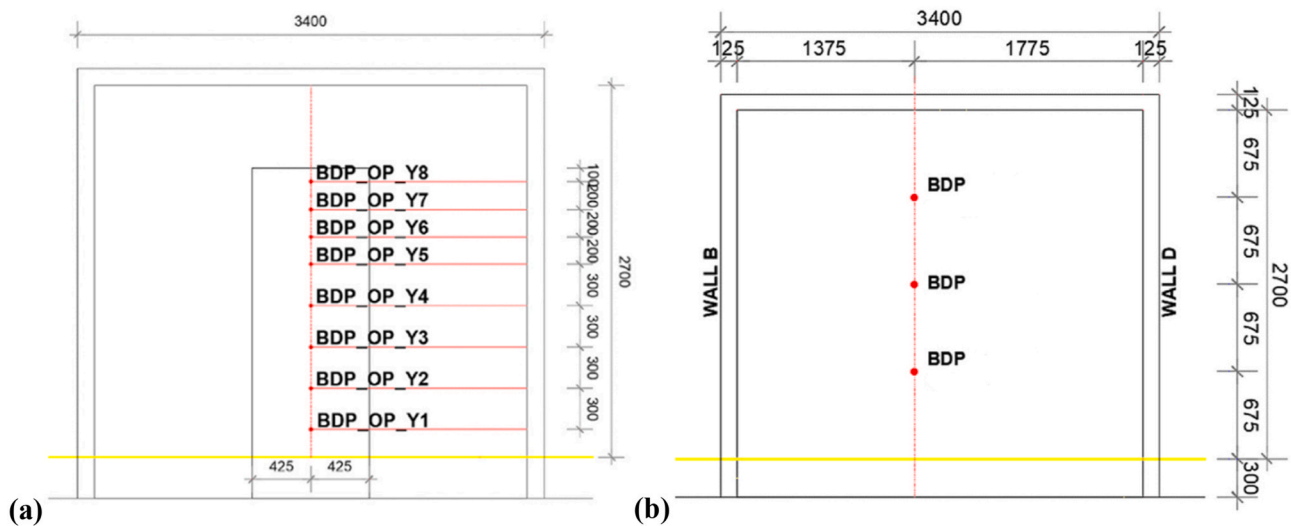


Fig. 3. (a) Locations of bi-directional probes and associated thermocouples at the opening, and (b) locations of internal bi-directional probes on the back wall.

they may have higher uncertainty for convective heating and during the cooling phase. However, this is not a significant issue in the current study of fully-developed fires where radiation is the dominant mode of heat transfer. Bi-directional velocity probes have also been shown to present difficulties of resolution at low velocities, and uncertainty of flow direction when the exact neutral plane height is variable or unknown [26]. In this study, velocity measurements are only used to compare the vertical flow fields between tests, and are corroborated by paired TC measurements.

3. Influence of exposed timber on the fully-developed fire dynamics

The phenomena of char fall-off, encapsulation failure, and self-extinguishment observed in these experiments are the subject of a planned three-part series of papers by the authors, beginning with Ref. [13]. As such, these phenomena are mentioned but not addressed in detail in this paper.

Flashover of the compartment occurred approximately 1 min after ignition of the pool fire in each case. Flashover was defined as the moment at which the average temperature at the top of the smoke layer reached 600 °C (measured by the top-most thermocouples at 2.36 m height). While this is a somewhat arbitrary definition, it is necessary to compare the fully-developed stage for each test. Therefore, the results were aligned in time such that $t = 0$ min corresponds to this moment.

Results and observations from each of the experiments show the influence of the exposed timber surfaces on the characteristics of the fire during the fully-developed phase. We have identified considerable differences between each experiment. This is noteworthy as this compartment geometry would ordinarily be classified as under-ventilated, and therefore the fire dynamics should be theoretically independent of the exposed timber. The experiments were characterised by a smoke layer that extended almost to the floor, with no visibility of the back or side walls of the compartment. Once the fire became fully-developed, the plume from the kerosene pool was tilted towards the back wall by the in-flowing air, with no appearance of a vertical buoyant plume. This was a consequence of the placement of the pool on the ground in front of the single ventilation opening, resulting in momentum driven flows as the incoming air velocities overcame the buoyancy forces of the plume. Similar tilting effects have also been observed by Hidalgo *et al.* [25], Hilditch [27] and Majdalani *et al.* [28].

3.1. Compartment temperatures

The internal temperature distributions and gradients in both horizontal and vertical directions are key to understanding the role of exposed timber surfaces on the compartment fire dynamics.

Approximately 4 min after flashover in all of the experiments, the median temperatures in the compartment reached a steady range of 1050–1150 °C, as shown in Fig. 4. For the comparison of gas temperatures during the fully-developed phase in each compartment, inter-quartile ranges in Fig. 4 (b) have been calculated over a 5 min period beginning 4 min after flashover. This ensures that all the fires were fully-developed throughout the period of comparison. Despite the similar median gas temperatures recorded during the fully-developed phase for all tests, there were wide differences in the spatial and temporal distributions of temperature in each case. This is not consistent with the characteristics of homogenous temperatures and heat fluxes for ventilation-controlled *Regime I* fires [10]. Moreover, the temperature distributions appear to be related to the configurations of exposed or encapsulated timber surfaces, as shown in Fig. 4. In the fully-encapsulated tests (Fig. 4 (a.1) and (a.2)), there was a varied distribution of temperatures from the front to the back of the compartment, with temperatures at the back of the compartment hundreds of degrees higher than at the front. Part of this difference can be attributed to the inflow of cool air near the lower thermocouples at the front, but even the highest thermocouples at the front recorded temperatures up to 200 °C below temperatures at the back. The primary cause of this spatial variation was the effect of the momentum-driven flows pushing the fuel-air mixture towards the rear of the compartment.

The introduction of an exposed lateral wall and ceiling (Fig. 4 (a.3) and (a.4)), appears to have altered the temperature distribution around the compartment, compared to the fully-encapsulated case. Instead of the previous front-to-back distribution of temperatures, the measurements from trees U, V, W, and Y did not maintain a consistent pattern in Test 2.1 and Test 2.2, and temperatures at each location shifted significantly and often suddenly. We hypothesize that the asymmetrical placement of the exposed wall D in these tests influenced the flow fields in the compartment, as production and combustion of pyrolysis gases from this wall (particularly in the lower part, where incoming oxygen is more available) created buoyant forces that induced vertical momentum on one side of the compartment. This additional momentum component could have in-turn affected the direction of tilt of the pool fire, while also creating vortices that result in heterogeneous temperature distributions (spatially and temporally). This hypothesis is consistent with the observations of Gorska *et al.* for medium-scale under-ventilated

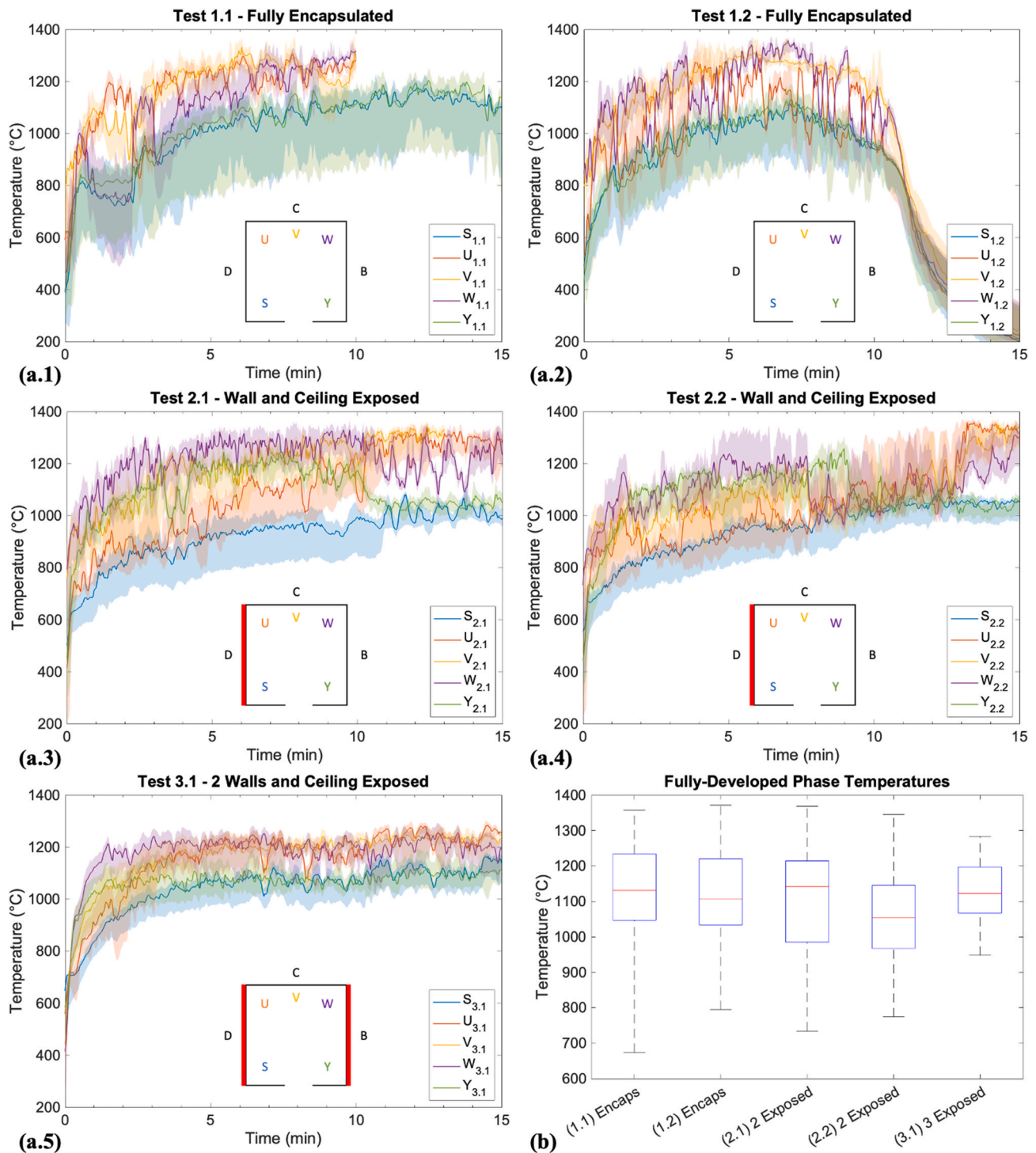


Fig. 4. (a) Median gas temperatures for each thermocouple tree in each test, with minimum and maximum temperature ranges shaded, and (b) comparison of temperature ranges for all tests during the fully-developed phase (4–9 min after flashover).

compartments [11] that the introduction of combustible walls promotes a momentum-driven regime that alters the velocity and temperature fields, with increased similarity to a *Regime II* or ‘fuel-surface-controlled’ fire [10].

In Test 3.1 with two lateral walls (B and D) and the ceiling (E) exposed (Fig. 4 (a.5)), there was a reversion to a more stable temperature distribution, with consistently higher temperatures towards the rear of the compartment. Although median temperatures for the whole compartment were similar to those in other tests, the interquartile range and distance between extreme values were narrower (Fig. 4 (b)). This is

explained firstly by the symmetry of the two exposed surfaces, which should promote symmetrical velocity and temperature fields. Secondly, the increased production of pyrolysis gases from the two combustible walls forces the smoke layer lower (see Section 3.2), which, combined with their location on either side of the pool, stalls the incoming air flow and redirects it laterally and vertically. This reduces the flow towards the back of the compartment and, consequently, the difference in temperature between the front and back of the compartment is reduced.

In all the tests with exposed timber, the combustible ceiling provided additional pyrolysis gases to the smoke layer. However, due to the

horizontalities of the ceiling, it would not contribute an additional positive vertical momentum component, but rather dampen the upwards flow of buoyant gases. In isolation, we expect this to promote hydrostatic conditions within the compartment, but the influence of the exposed ceiling was not de-coupled from that of the exposed walls in this experimental series, so this hypothesis requires confirmation.

Analysis of the vertical temperature distributions in each compartment provides further evidence of the impact of exposed timber surfaces on the fire dynamics. For the same fully-developed period of 4–9 min post-flashover, median vertical temperature profiles at the front and back of the compartment for each experiment are presented in Fig. 5. For the encapsulated tests, median temperatures at the back were relatively uniform, exceeding 1200 °C for the full height of the compartment. Near the front, temperatures were 100–400 °C lower and there was a pronounced vertical gradient, with temperatures increasing monotonically from bottom to top. Again, this is consistent with the effect of the kerosene vapour plume being driven strongly towards the back wall. In comparison, temperatures towards the front for all tests with exposed surfaces displayed a distinct curved gradient, with temperatures reaching a maximum around the mid-height and decreasing towards the top. This effect was also observed by Gorska *et al.* [11], and is caused by the additional pyrolysis gases from the exposed walls and ceiling pushing the neutral plane at the doorway lower (see Section 3.2) and creating a particularly fuel-rich region beneath the ceiling that reduces temperatures at the top of the compartment. For the same reasons, temperatures at the back for tests 2.1 and 2.2 reached a maximum between 0.6 and 1.2 m above floor level, before decreasing towards the ceiling.

In Test 3.1, near the front, temperatures in the lower half of the compartment were higher than in all other tests, and were comparatively closer in range to the temperatures in the top half of the compartment. This provides further evidence that the two exposed lateral walls reduced the velocity of airflow towards the back of the compartment, allowing more combustion to occur closer to the front. Consistent with this explanation, temperatures at the back in the bottom half of the compartment for Test 3.1 were up to 100 °C lower than for the encapsulated tests, as the combusting kerosene vapour was no longer being driven backwards as strongly. Temperatures at the back gradually increased with height, due to the buoyant flows generated by the combusting walls, before decreasing again below the ceiling.

3.2. Fire-induced flow fields

In order to calculate the inflow and outflow velocities in the doorway, voltage signals from the differential pressure transducers

coupled to the bi-directional probes were converted to velocities by applying the probe-transducer assembly corrections and methodology of Gupta [23]. Density corrections for temperature were performed with the use of local thermocouple measurements adjacent to each probe (see Fig. 3). The average velocity over the 5 min fully-developed period for the doorway probes in each experiment is shown in Fig. 6 (a). Average temperatures corresponding to the location of each of the BDPs are shown in Fig. 6 (b).

The flow results in Fig. 6 (a) show that the neutral plane position ($V = 0$) appears to shift downwards from ~1 m to 0.65 m with an increased exposed surface area of timber. The reduction of neutral plane height with A_e shows that the additional hot pyrolysis gases due to the exposed surfaces increase the velocities of the outflow (and mass flux). It is interesting to observe an overall reduction in the inflow velocities as A_e/A_T increases. This suggests that the so-called “pump” effect of the fire plume [27], which draws in air towards the pool and results in the plume tilting, is inhibited by the lateral flows and reduced neutral plane height induced by the burning walls. Larger temperatures are observed at the opening in Fig. 6 (b) as A_e/A_T increases, indicating that excess pyrolyzates released from the exposed walls burn at the doorway plume.

The temperature profiles at the doorway, shown in Fig. 6 (b), are a useful indicator of the thermal interface height and can be used to infer the projection of the flame by tracking temperatures that approach the characteristic bulk fire temperature (~1100 °C). The thermocouples below the neutral plane at the door recorded temperatures far above ambient level due to radiative heat transfer, since no correction for this was applied (as explained in Section 2). Nonetheless, these measurements reliably indicate the locations of hotter and colder regions. The experiments with combustible walls (tests 2.1, 2.2 and 3.1) show distinct peak temperatures between 1.4 and 1.8 m, with the temperatures decreasing towards the top of the doorway. As the exposed surfaces increase, the flame projection height (inferred using the thermocouple profiles) through the doorway appears to decrease from approximately 1.8–2.0 m to 1.4–1.6 m. This observation tracks well with the down-shifting of the neutral plane height, and is consistent with the existence of a more fuel-rich layer near the top of the compartment, promoted by the exposed surfaces.

To understand the effects of the burning walls on the internal flow fields, summary statistics of the internal bi-directional flow measurements on the back wall (C) are shown in Fig. 7. Three different sampling points are shown on the back wall in Fig. 7, corresponding to vertical elevations of $z = 0.68$ m, $z = 1.35$ m, and $z = 2.03$ m. Contrasting the tests highlights the considerably larger positive (upwards) flow velocities at the back wall for the completely encapsulated tests at all three

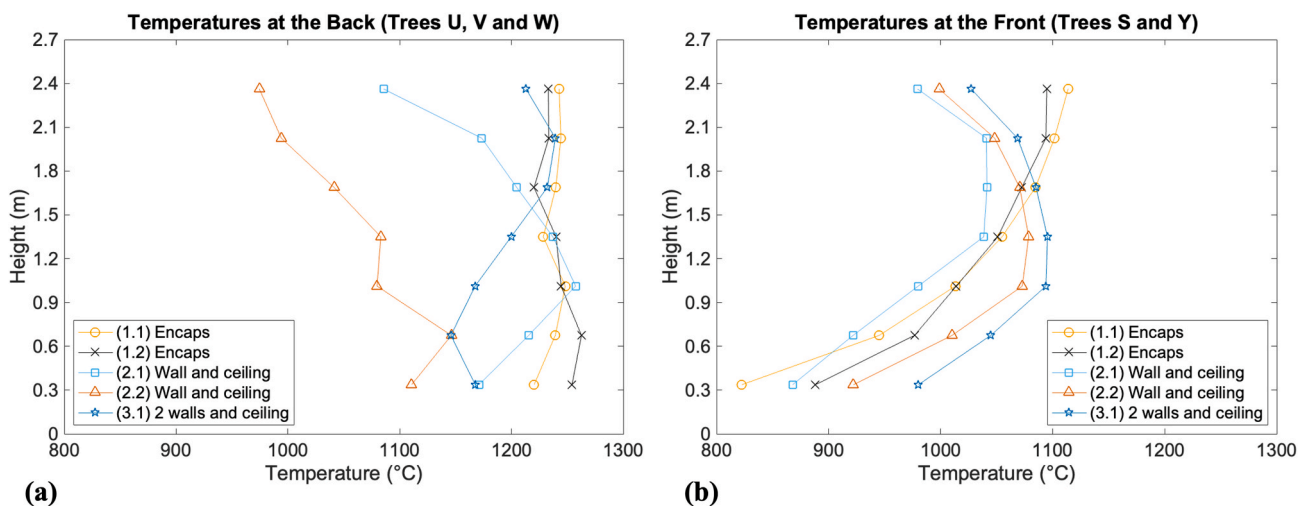


Fig. 5. Distribution of internal temperatures towards (a) the back, and (b) the front of the compartment in each experiment – averaged for the specified groups of thermocouple trees over the fully-developed period (4–9 min after flashover).

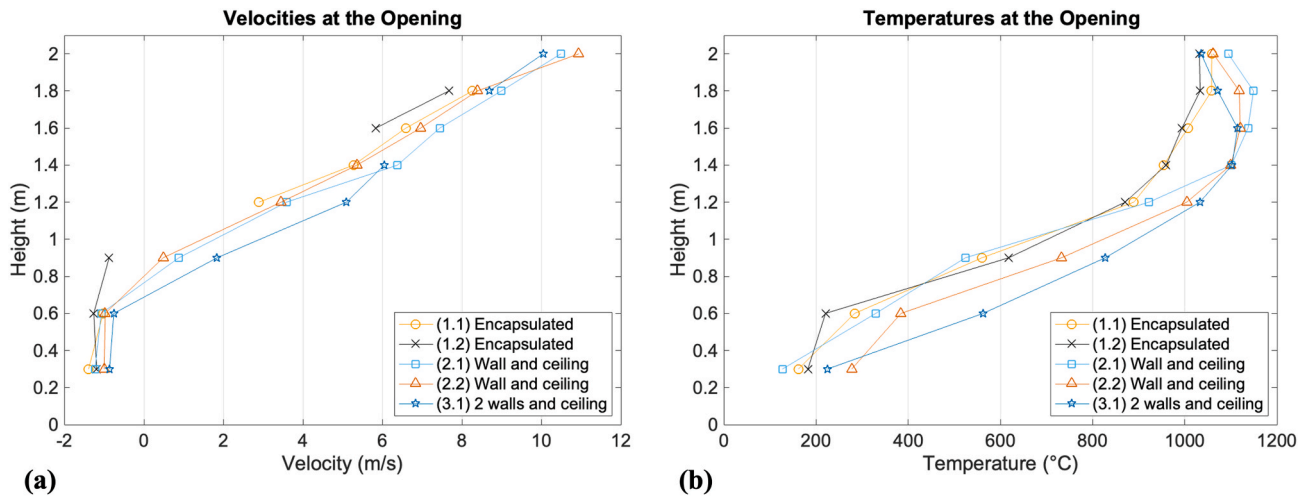


Fig. 6. Distribution of average (a) velocities, and (b) temperatures over the height of the opening.

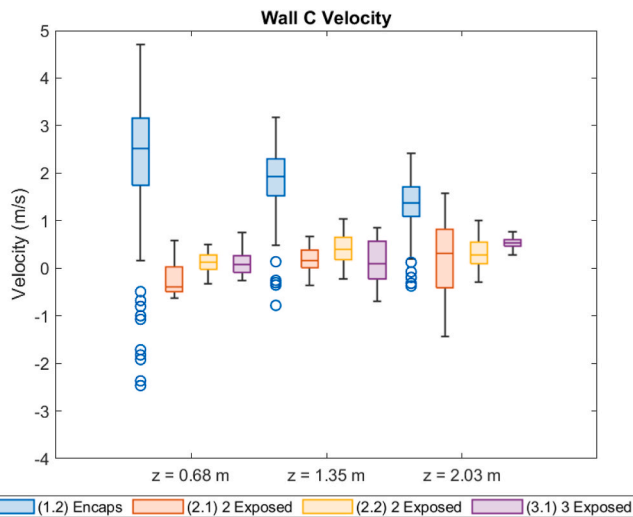


Fig. 7. Measurements of internal velocity from BDPs at different heights on the back wall during the fully-developed period (4–9 min after flashover). Upward velocities are positive.

elevations. This is linked to the plume tilting effect that occurred due to the entrained inflow resulting in significant momentum generation along the length of the back wall. In contrast, exposing the timber walls significantly stalled the flow field along the back wall irrespective of A_e/A_T , with mean axial velocities typically ranging between -0.5 m/s to 0.5 m/s, indicating flow recirculation. This suggests that the fire plume was no longer tilted towards the back wall, with the pool fire burning in a more buoyant manner. This was likely associated to a larger proportion of air entrained into the compartment being directed laterally, towards the exposed flaming walls, thereby reducing the overall momentum of the inflow directed at the primary fire plume. The considerably larger error bars shown on the plot also demonstrate the large turbulent fluctuations that took place for the fully-encapsulated test, where momentum-dominated flows were most prevalent. These fluctuations were dampened considerably by the addition of exposed timber, showing the stabilising effect of the lateral burning timber walls on the back wall flows.

The fire dynamics in each compartment are fundamentally linked to the boundary heat fluxes, which are essential for analysis of the structural performance and related phenomena, such as encapsulation failure and char fall-off. The relationships between the different fire dynamics

described in this section and the associated heat fluxes to the boundaries are explored in the following section.

4. Influence of exposed timber on heat fluxes to the boundaries

The imposed radiative heat flux on the compartment boundaries is a useful quantity to study as it amalgamates the compartment fire dynamics into a thermal boundary condition. Therefore, this quantity enables a spatial mapping of localised heat release zones and hot areas in the compartment.

Considerable spatial distributions of the incident radiative heat fluxes were apparent in all experiments, with the quantity of exposed timber surfaces having a large influence on the heating of different surfaces in the compartment. Fig. 8 (a) shows the median, 25th percentile and 75th percentile incident radiant heat fluxes measured in different experiments. Heat fluxes were not measured in Test 1.1, out of a desire to avoid accelerating failure of the encapsulation due to damage from embedding TSCs. Calculation of the incident radiant heat flux from TSC measurements was conducted according to the method described by Hidalgo *et al.* [21].

For comparison of fully-developed conditions between tests, the heat flux ranges shown in Figs. 8 (b) and Fig. 9 have been calculated for the same 5 min period used in Section 3, beginning 4 min after flashover. During this comparison period, overall heat fluxes in the compartment were similar for the fully-encapsulated Test 1.2 and Test 2.2 with one wall and the ceiling exposed, with interquartile ranges between 50 and 150 kW/m². In Test 3.1 with three exposed surfaces, the overall median and IQR were 25 – 50 kW/m² higher, but the peak heat flux measured in this period was similar to the other cases, at approximately 280 kW/m². In Fig. 8 (a), it can be seen that heat fluxes in Test 2.2 and 3.1 continue to increase until 15 min after flashover, reaching median heat flux values in the range of 150 – 200 kW/m². Throughout this time, median heat fluxes were consistently higher by ~ 50 kW/m² for Test 3.1 with a greater area exposed.

Comparison of the heat flux ranges on the back wall (C) and ceiling (E) for each test in Fig. 8 (b) demonstrates how exposed timber surfaces can affect the spatial distributions of thermal boundary conditions even in under-ventilated compartments. For the back wall, the highest range of heat fluxes was for the fully-encapsulated test, related to the strong momentum-driven flows forcing the burning fuel towards the rear. As explained in Section 3, this flow field is disturbed by the introduction of combustible walls, leading to wider but generally lower ranges at the back wall for Test 2.2 and Test 3.1. At the ceiling, the presence of an additional combustible wall in Test 3.1 appears to increase the heat fluxes, with median values around 50 kW/m² higher than for the other

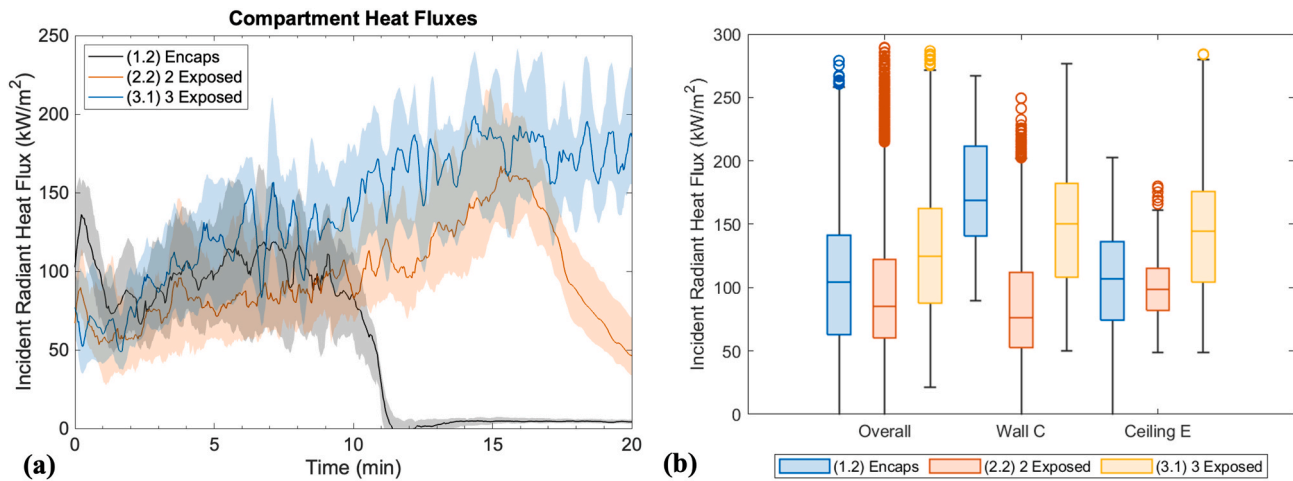


Fig. 8. (a) Temporal evolution of medians (solid lines) and interquartile ranges (shaded) of incident radiant heat fluxes in each compartment, and (b) comparison of heat flux ranges during the fully-developed period (4–9 min after flashover).

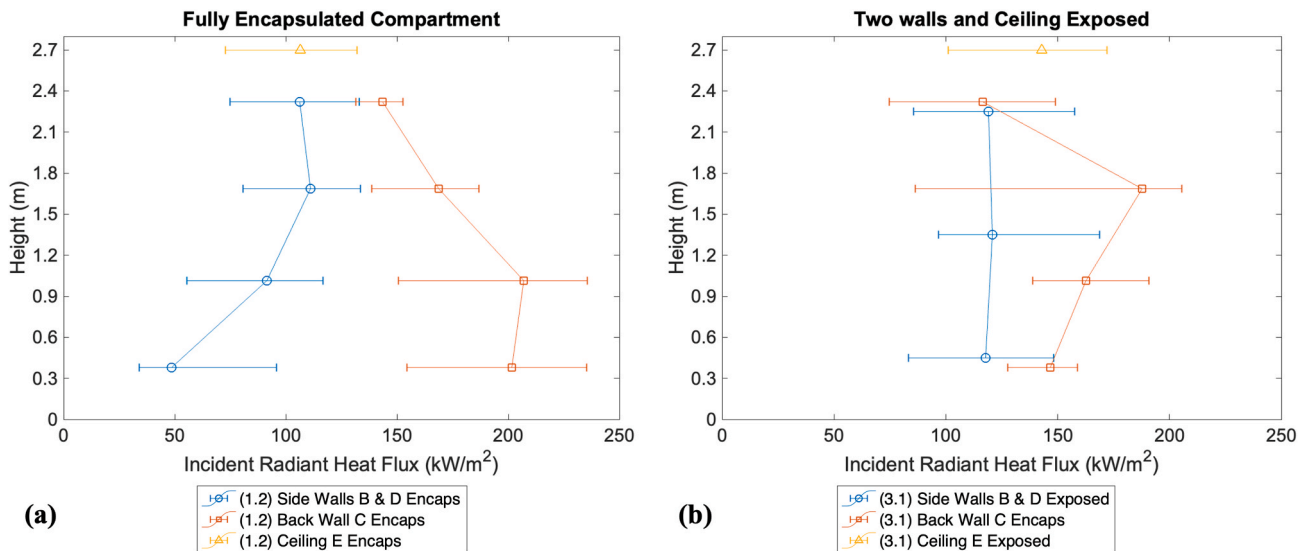


Fig. 9. Distribution of heat fluxes to the boundaries in (a) fully encapsulated Test 1.2, and (b) Test 3.1 with two walls and the ceiling exposed. Error bars represent interquartile ranges.

tests. This also supports the notion that the very high production of pyrolysis gases by the exposed walls on each side of the pool, as well as the ceiling, combine to stall the flow towards the back of the compartment, and redirect it upwards due to buoyancy.

The effect of the exposed surfaces on the vertical heat flux distribution is shown in Fig. 9 for Test 1.2 (fully-encapsulated) and Test 3.1 (three exposed surfaces). The error bars represent the limits of the interquartile range, and encompass the local spatial distribution of heat flux sensors for each surface.

Heat flux distributions appear to be more uniform vertically for Test 3.1, while the large error bars at each height explicitly show large fluctuations (even exceeding 100 kW/m^2) in localised heating occurring due to the presence of burning timber walls. This is expected given that the two vertical burning walls exhibit turbulent boundary layer behaviour, which induces significant upward momentum in the compartment. Interestingly, the incident radiant heat flux at the ceiling is $30\text{--}40 \text{ kW/m}^2$ higher for Test 3.1 than for the fully-encapsulated Test 1.2. These results are quite different to the medium-scale experiments of Gorska *et al.* [11], where the additional mass flux of fuel from exposed timber surfaces was postulated to have created a region of less efficient combustion beneath the ceiling, which increases soot formation and the

stabilisation of an opaque smoke layer. Ceiling heat fluxes for Test 3.1 were also observed to be consistent with heat fluxes closer to the floor. At this larger scale, it appears that the strong buoyant flow of combustion products towards the ceiling, caused by the large area of exposed timber walls, dominates over the formation of a stable smoke layer that would otherwise insulate the ceiling from radiative heat transfer.

The heat fluxes for the burning timber walls (walls B and D) in Test 3.1 are shown in Fig. 9 (b) to be relatively uniform, despite the turbulent boundary layer flows established over the surface of the walls. This indicates that radiative heat transfer external to the wall from other burning surfaces, the smoke layer, and the pool fire controlled the heat transfer and burning rates of each vertical wall rather than local convective flows. Given the large-scale nature of the experiment, radiative heat transfer is expected to predominate over convection, which has also been observed in large open-plan compartment fire experiments [19]. Encapsulated side walls, particularly lower in the compartment, have much lower heat fluxes of as little as 50 kW/m^2 , which again highlights the strong role of radiation with the presence of vertical timber walls. The location of the peak back wall heat flux increased from $z = 0.9 \text{ m}$ in Test 1.2 to $z = 1.6 \text{ m}$ in Test 3.1, suggesting that the plume tilting effect that was prominent for the fully encapsulated test is

weakened by the exposed lateral walls.

Together, these variations in spatial heat fluxes clearly show the influence of the exposed timber surfaces and fuel nature on the fire dynamics within the compartment – despite the geometry of the compartment being classically described as ventilation-limited. Nevertheless, the heat flux ranges observed in all of these compartment fires ($\sim 50\text{--}250\text{ kW/m}^2$) are comparable to those recorded for other large-scale under-ventilated compartments [16].

5. Implications for mass timber structures

Consideration of the analysis presented in Sections 3 and 4 leads to several important consequences for fire safety engineering methodologies applied to exposed mass timber structures:

- Even for ‘under-ventilated’ compartments, exposed timber compartments do not exhibit a homogeneous thermal environment. There can be wide ranges of heat flux spatially and temporally. It has been shown that the spatial distributions of localised heating heavily depend on A_e/A_T and also the particular geometry of exposed surfaces (i.e., horizontal ceilings or vertical walls).
- Vertical momentum is added by the combusting boundary layer flows established over the exposed vertical timber walls. As the area of exposed walls increases, this high-inertia flow impinges on the ceiling, creating localised flow recirculation that promotes turbulent mixing and combustion. This results in larger heat fluxes to the ceiling and invalidates the assumption of a stagnant, poorly-mixed layer beneath the ceiling that was previously identified by Gorska *et al.* [11] for reduced-scale compartments.
- Due to the large temperature distributions and internal velocity gradients, assumptions of uniform mixing and hydrostatic flows, commonly used to analyse under-ventilated compartments, do not hold applicability at this scale. This finding applies to both the fully-encapsulated and exposed timber compartments; however, the internal fire dynamics vary significantly with changes to A_e/A_T and the configuration of exposed surfaces.
- This is likely to be even more critical for *Regime II* compartment typologies with exposed vertical walls, due to the combination of additional fuel and high momentum flows with greater oxygen availability. Moreover, the combustion of large timber surfaces in well-ventilated compartments can lead to accelerated flame spread and transition to fully-developed fire due to higher radiation feedback to the fuel bed [19,24,29]. Consequently, the assumption of generally less onerous thermal environments for *Regime II* compartments [30] may not be valid.
- Maximum gas temperatures exceed the predictions for under-ventilated compartment fires utilising the opening factor [10]. Nevertheless, both the fully-encapsulated and exposed timber tests exhibit a range of radiative heat fluxes that are consistent with other fully-developed large-scale compartments of $50\text{--}250\text{ kW/m}^2$ [16].
- Despite similar ranges of thermal conditions inside the compartment, particular consideration of the external plume should be employed. It has been shown that outflow velocities and temperatures increase with A_e/A_T due to excess fuel production and momentum generation from the burning exposed walls. This will undoubtedly create more severe heating conditions on the external façade, as found also by Gorska *et al.* and Sjöström *et al.* [11,31,32], with implications for maintaining vertical compartmentation.
- Consequently, design tools that invoke the assumptions discussed here should be employed cautiously and used with a high degree of conservatism that encompasses the uncertainty and wide range of heat flux distributions observed in reality. Localised heat distributions are particularly important in timber compartments due to the potential for local hot spots that can promote failure modes such as char fall-off and encapsulation failure, which can add to the overall heat release rate of the compartment fire, and also inhibit self-

extinguishment [1–3,5,11]. Spatially resolved tools such as computational fluid dynamics codes can also benefit from the insights of this paper to establish their capability to model the complex momentum and heat transfer processes observed.

6. Conclusions

The increasing use of mass timber in construction necessitates a re-evaluation of common assumptions and methodologies for describing compartment fire dynamics when these timber surfaces are exposed. This study demonstrates the effects of combustible surfaces on the fully-developed fire dynamics in large-scale under-ventilated mass timber compartments. The experimental results highlight the inadequacy of the conventional *compartment fire framework* in describing the thermal exposures that influence the performance of engineered timber. All the compartments studied were of a geometry and opening factor that would conventionally define them as ventilation-controlled, or *Regime I*, and therefore, unaffected by the nature and configuration of the fuel load. Instead, significant variations were seen in the fire dynamics and resulting distributions of heat flux within each compartment, and between compartments with different areas and configurations of exposed surfaces. The following conclusions can be drawn:

- Increasing the surface area of exposed timber in the compartment alters the internal flow fields and velocity magnitudes. The mechanism driving this is linked to the burning vertical walls that create combusting turbulent boundary layer flows, which add a local vertical momentum component. These burning walls also drive the neutral plane lower and draw some of the inflowing air towards them, thereby stalling the inflow directed towards the kerosene fuel plume. This has the effect of reducing the plume tilt towards the back wall.
- The flow at the doorway does not choke or reach a limiting condition despite a continually descending neutral plane height with increases in the exposed surface area of timber. The outflow velocities increase with the area of exposure due to the additional pyrolysis gases generated, while inflows decrease slightly due to the previously mentioned stalling effect.
- The complex momentum-driven flow fields control the temperature fields and radiative heat fluxes imposed onto the compartment boundaries. Spatial distributions (both horizontally and vertically) and temporal evolutions of heating within the compartment are highly heterogeneous and dependent on the configuration of exposed timber surfaces. This contradicts the conventional assumptions of thermal conditions for under-ventilated compartment fires being relatively homogeneous and governed by the opening factor.
- These findings demonstrate the importance of having a sufficient resolution of instrumentation in compartment fire experiments to adequately resolve the spatial distributions in the thermal environment.

The results show that resolution of the fire-induced flows from both the moveable fuel load and the exposed timber walls is a first order parameter that controls the fully-developed phase of large-scale compartment fires with exposed timber walls. Typical simplifications of the momentum equation in zone models, which are commonly used to define thermal boundary conditions in under-ventilated compartments, are not valid in mass timber compartments. The thermal boundary conditions in the fully-developed phase dictate the level of structural damage and can induce localised failures, such as char fall-off or encapsulation failure, which can inhibit self-extinction. Therefore, these simplified solutions should be used in a conservative manner that accounts for the range of thermal conditions observed in large-scale experiments.

Declaration of competing interest

The authors declare the following financial interests/personal relationships which may be considered as potential competing interests: Juan P. Hidalgo reports equipment, drugs, or supplies was provided by Queensland Fire and Emergency Services. Juan P. Hidalgo reports equipment, drugs, or supplies was provided by XLam. Juan P. Hidalgo reports equipment, drugs, or supplies was provided by Hyne Timber. Juan P. Hidalgo reports equipment, drugs, or supplies was provided by Lendlease. Juan P. Hidalgo reports equipment, drugs, or supplies was provided by Knauf. Juan P. Hidalgo reports equipment, drugs, or supplies was provided by Rockwool International. Editorial board member of the journal (Fire Safety Journal) - David Lange. Editorial board member of the journal (Fire Safety Journal) - Felix Wiesner. Editorial board member of the journal (Fire Safety Journal) - Juan P. Hidalgo.

Data availability

Data will be made available on request.

Acknowledgements

This project was funded by the ARC Future Timber Hub (IH150100030) and received generous support from QFES, XLam, Hyne Timber, Lend Lease, Knauf and Rockwool International A/S. The authors are extremely grateful to QFES for providing their research facility and engagement with the project. Dr Pope is supported by the Innovation Fund Denmark, the Danish Agency for Higher Education and Science, and DBI. Staff and students helping with the project are gratefully acknowledged: A. Bolanos, A. Browning, J. Cadena, J. Carrascal, E. Candansayar, P. Chowdhury, J. Cuevas, C. Gorska, M. Griffith, M. Hewitt, T. Iturralde, M. Javidnejad, G. Kanellopoulos, A. Lucherini, C. Maluk, S. Matthews, M. McLaggan, J. Mendez, A.F. Osorio, L. Ramadhan, A. Solarte, D. Soriguer, D. Tanudirdjo, W. Wu, H. Wyn, A. Zaben, YH. Zhang and YS. Zhu.

References

- [1] X. Li, X. Zhang, G. Hadjisophocleous, C. McGregor, Experimental study of combustible and non-combustible construction in a natural fire, *Fire Technol.* 51 (2015) 1447–1474, <https://doi.org/10.1007/s10694-014-0407-4>.
- [2] R.M. Hadden, A.I. Bartlett, J.P. Hidalgo, S. Santamaria, F. Wiesner, L.A. Bisby, S. Deeny, B. Lane, Effects of exposed cross laminated timber on compartment fire dynamics, *Fire Saf. J.* 91 (2017) 480–489, <https://doi.org/10.1016/j.firesaf.2017.03.074>.
- [3] A.I. Bartlett, R.M. Hadden, J.P. Hidalgo, S. Santamaria, F. Wiesner, L.A. Bisby, S. Deeny, B. Lane, Auto-extinction of engineered timber: application to compartment fires with exposed timber surfaces, *Fire Saf. J.* 91 (2017) 407–413, <https://doi.org/10.1016/j.firesaf.2017.03.050>.
- [4] R. Emberley, C.G. Putynska, A. Bolanos, A. Lucherini, A. Solarte, D. Soriguer, M. G. Gonzalez, K. Humphreys, J.P. Hidalgo, C. Maluk, A. Law, J.L. Torero, Description of small and large-scale cross laminated timber fire tests, *Fire Saf. J.* 91 (2017) 327–335, <https://doi.org/10.1016/j.firesaf.2017.03.024>.
- [5] J. Su, P.-S. Lafrance, M. Hoehler, M. Bundy, Fire Safety Challenges of Tall Wood Buildings - Phase 2: Task 3 - Cross Laminated Timber Compartment Fire Tests, National Institute of Standards and Technology, 2018, <https://doi.org/10.18434/T4/1422512>.
- [6] D. Brandon, J. Sjöström, E. Hallberg, A. Temple, F. Kahl, Fire Safe Implementation of Visible Mass Timber in Tall Buildings – Compartment Fire Testing, RISE, 2020.
- [7] R. McNamee, J. Zehfuss, A.I. Bartlett, M. Heidari, F. Robert, L.A. Bisby, Enclosure fire dynamics with a cross-laminated timber ceiling, *Fire Mater.* 45 (2021) 847–857, <https://doi.org/10.1002/fam.2904>.
- [8] F. Wiesner, A. Bartlett, S. Mohaine, F. Robert, R. McNamee, J.-C. Mindeguia, L. Bisby, Structural capacity of one-way spanning large-scale cross-laminated timber slabs in standard and natural fires, *Fire Technol.* 57 (2021) 291–311, <https://doi.org/10.1007/s10694-020-01003-y>.
- [9] P.H. Thomas, A.J.M. Heselden, M. Law, Fully-developed Compartment Fires - Two Kinds of Behaviour, 1967.
- [10] J.L. Torero, A.H. Majdalani, C. Abecassis-Empis, A. Cowlard, Revisiting the compartment fire, *Fire Saf. Sci.* 11 (2014) 28–45, <https://doi.org/10.3801/IAFSS.FSS.11-28>.
- [11] C. Gorska, J.P. Hidalgo, J.L. Torero, Fire dynamics in mass timber compartments, *Fire Saf. J.* 120 (2020), 103098, <https://doi.org/10.1016/j.firesaf.2020.103098>.
- [12] D.I. Kolaitis, E.K. Asimakopoulou, M.A. Founti, Fire protection of light and massive timber elements using gypsum plasterboards and wood based panels: a large-scale compartment fire test, *Construct. Build. Mater.* 73 (2014) 163–170, <https://doi.org/10.1016/j.conbuildmat.2014.09.027>.
- [13] H. Xu, I. Pope, V. Gupta, J. Cadena, J. Carrascal, D. Lange, M.S. McLaggan, J. Mendez, A. Osorio, A. Solarte, D. Soriguer, J.L. Torero, F. Wiesner, A. Zaben, J. P. Hidalgo, Large-scale compartment fires to develop a self-extinction design framework for mass timber—Part 1: literature review and methodology, *Fire Saf. J.* 128 (2022), 103523, <https://doi.org/10.1016/j.firesaf.2022.103523>.
- [14] I. Pope, H. Xu, V. Gupta, J. Carrascal, D. Lange, M. McLaggan, J. Mendez, A. Solarte, D. Soriguer, J.L. Torero, F. Wiesner, J.P. Hidalgo, Fire dynamics in under-ventilated mass timber room compartments, in: Proc. 12th Asia-Ocean. Symp. Fire Sci. Technol. AOSFST 2021, The University of Queensland, Online, 2021, <https://doi.org/10.14264/7e19a8f>.
- [15] J. Liu, E.C. Fischer, Review of large-scale CLT compartment fire tests, *Construct. Build. Mater.* 318 (2022), 126099, <https://doi.org/10.1016/j.conbuildmat.2021.126099>.
- [16] V. Gupta, J.P. Hidalgo, D. Lange, A. Cowlard, C. Abecassis-Empis, J.L. Torero, A review and analysis of the thermal exposure in large compartment fire experiments, *Int. J. High-Rise Build.* 10 (2021) 345–364, <https://doi.org/10.21022/IJHRB.2021.10.4.345>.
- [17] C. Wade, M. Spearpoint, C. Fleischmann, G. Baker, A. Abu, Predicting the fire dynamics of exposed timber surfaces in compartments using a two-zone model, *Fire Technol.* 54 (2018) 893–920, <https://doi.org/10.1007/s10694-018-0714-2>.
- [18] D. Brandon, A. Temple, J. Sjöström, Predictive Method for Fires in CLT and Glulam Structures – A Priori Modelling versus Real Scale Compartment Fire Tests & an Improved Method, RISE, 2021.
- [19] V. Gupta, J.L. Torero, J.P. Hidalgo, Burning dynamics and in-depth flame spread of wood cribs in large compartment fires, *Combust. Flame* 228 (2021) 42–56, <https://doi.org/10.1016/j.combustflame.2021.01.031>.
- [20] N. Tondini, J.-M. Franssen, Analysis of experimental hydrocarbon localised fires with and without engulfed steel members, *Fire Saf. J.* 92 (2017) 9–22, <https://doi.org/10.1016/j.firesaf.2017.05.011>.
- [21] J.P. Hidalgo, C. Maluk, A. Cowlard, C. Abecassis-Empis, M. Krajcovic, J.L. Torero, A Thin Skin Calorimeter (TSC) for quantifying irradiation during large-scale fire testing, *Int. J. Therm. Sci.* 112 (2017) 383–394, <https://doi.org/10.1016/j.jthermalsci.2016.10.013>.
- [22] S. Welch, A. Jowsey, S. Deeny, R. Morgan, J.L. Torero, BRE large compartment fire tests—characterising post-flashover fires for model validation, *Fire Saf. J.* 42 (2007) 548–567, <https://doi.org/10.1016/j.firesaf.2007.04.002>.
- [23] V. Gupta, Open-plan compartment fire dynamics, in: PhD Thesis, The University of Queensland, 2021, <https://doi.org/10.14264/d35999e>.
- [24] J.P. Hidalgo, T. Goode, V. Gupta, A. Cowlard, C. Abecassis-Empis, J. Maclean, A. I. Bartlett, C. Maluk, J.M. Montalvá, A.F. Osorio, J.L. Torero, The Malveira fire test: full-scale demonstration of fire modes in open-plan compartments, *Fire Saf. J.* 108 (2019), 102827, <https://doi.org/10.1016/j.firesaf.2019.102827>.
- [25] J.P. Hidalgo, A. Cowlard, C. Abecassis-Empis, C. Maluk, A.H. Majdalani, S. Kahrman, R. Hilditch, M. Krajcovic, J.L. Torero, An experimental study of full-scale open floor plan enclosure fires, *Fire Saf. J.* 89 (2017) 22–40, <https://doi.org/10.1016/j.firesaf.2017.02.002>.
- [26] V. Gupta, C. Maluk, J.L. Torero, J.P. Hidalgo, Analysis of convective heat losses in a full-scale compartment fire experiment, in: Proc. Ninth Int. Semin. Fire Explos. Hazards ISFEH9, Saint Petersburg, Russia, 2019, pp. 490–501, <https://doi.org/10.18720/SPBPU/2/K19-53>.
- [27] R.R. Hilditch, Smoke Management for Modern Infrastructure, The University of Edinburgh, 2017.
- [28] A.H. Majdalani, J.E. Cadena, A. Cowlard, F. Munoz, J.L. Torero, Experimental characterisation of two fully-developed enclosure fire regimes, *Fire Saf. J.* 79 (2016) 10–19, <https://doi.org/10.1016/j.firesaf.2015.11.001>.
- [29] S. Nothard, D. Lange, J.P. Hidalgo, V. Gupta, M.S. McLaggan, F. Wiesner, J. L. Torero, Factors influencing the fire dynamics in open-plan compartments with an exposed timber ceiling, *Fire Saf. J.* 129 (2022), 103564, <https://doi.org/10.1016/j.firesaf.2022.103564>.
- [30] A.H. Majdalani, J.E. Cadena, A. Cowlard, F. Munoz, J.L. Torero, Experimental characterisation of two fully-developed enclosure fire regimes, *Fire Saf. J.* 79 (2016) 10–19, <https://doi.org/10.1016/j.firesaf.2015.11.001>.
- [31] C. Gorska, Fire dynamics in multi-scale timber compartments, in: PhD Thesis, The University of Queensland, 2020, <https://doi.org/10.14264/uql.2020.795>.
- [32] J. Sjöström, D. Brandon, A. Temple, J. Anderson, R. McNamee, External fire plumes from mass timber compartment fires—comparison to test methods for regulatory compliance of façades, *Fire Mater.* 47 (2023) 433–444, <https://doi.org/10.1002/fam.3129>.